Acta metall. mater. Vol. 42, No. 2, pp. 365–381, 1994
Printed in Great Britain.

0956-7151/94 $6.00 + 0.00

OVERVIEW NO. 112

THE CYCLIC PROPERTIES OF ENGINEERING MATERIALS

N. A. FLECK[1], K. J. KANG[2] and M. F. ASHBY[1]

[1]Cambridge University Engineering, Trumpington Street, Cambridge CB2 1PZ, England and
[2]Department of Mechanical Engineering, Chonnam National University, Kwangju 500-757, Republic of Korea

(Received 12 July 1993)

Abstract—The basic fatigue properties of materials (endurance limit, fatigue threshold and Paris law constants) are surveyed, inter-related and compared with static properties such as yield strength and modulus. The properties are presented in the form of *Material Property Charts*. The charts identify fundamental relationships between properties and, when combined with *performance indices* (which capture the performance-limiting grouping of material properties) provide a systematic basis for the optimal selection of materials in fatigue-limited design.

1. INTRODUCTION

1.1. Materials property charts and performance indices

The enormous range of engineering materials is conventionally subdivided into six classes: metals, ceramics, glasses, polymers, elastomers and, finally, composites made by combining two or more of the others. There is logic in this: properties, often, are similar within a class; between classes they differ. Metals, for instance, are stiff, tough and conduct heat well; polymers are compliant, relatively brittle and poor conductors. An earlier paper [1] surveyed the static mechanical and thermal properties of engineering material, presenting them as *material property charts*. Such charts have intrinsic value in revealing correlations and in displaying the relationship between the properties of the six classes; and they have practical application as a tool for rational material selection in design. In this paper we extend the method to the cyclic mechanical properties.

A material property chart is a diagram with one or a combination of material properties as its axes, on which the fields occupied by each material class and of the individual members within each class are plotted. Figure 1 illustrates the idea. In this schematic the axes are the endurance or fatigue limit, σ_e (defined in a moment), and the density, ρ. Data for members of a class cluster together, allowing them to be enclosed by class-envelopes (heavy boundaries). The class envelopes may overlap, but they nontheless occupy a characteristic position on the chart: on this one, ceramics lie near the top right, foams near the bottom left. Almost always, further information can be displayed. On Fig. 1, the specific endurance limit, σ_e/ρ, is shown on a set of diagonal contours, parallel, because of the logarithmic scales of the axes. In the design of light, fatigue-resistant structures the ratio σ_e/ρ often appears.

Of the many uses of such charts, two will be emphasised here. First, they reveal correlations between material properties that suggest fundamental relationships, helpful both in understanding and in estimating and checking property data; and second, when combined with *performance indices*, they form the basis of a rational procedure of material selection in mechanical design [1, 2].

A performance index is a combination of material properties which, if maximised, maximises some aspect of the performance of a component. One has appeared already: the best materials for making a light, fatigue-resistant, tie (a tensile member) are those with high values of the specific endurance limit, σ_e/ρ. There are others involving σ_e and ρ: the best materials for a light, fatigue-resistant beam, loaded in bending, are those with high values of $\sigma_e^{2/3}/\rho$; for a light fatigue-resistant panel in bending it is $\sigma_e^{1/2}/\rho$. Many such indices are known; they are the key to optimising material selection when weight or cost are to be minimised, or some aspect of performance is to be maximised. A compilation of indices for static properties can be found in Ref. [2]; one for cyclic properties is given here as Table 1.

1.2. Data sources and assumptions

The data plotted on the charts of this paper have been assembled from a wide variety of sources. Much use has been made of original publications, and the data have been cross-checked where possible. The charts show a *range* of properties for each material. For *structure-insensitive* properties—density, for example—the range is narrow. For *structure-sensitive* properties—endurance limit, for instance—it is wider, reflecting the range made available by heat treatment

Table 1. Performance indices for fatigue

(a) Infinite life design at minimum weight (cost, energy)[a]; uncracked samples

Component shape and loading[b]	Maximise
Tie (tensile strut). Cyclic load and length specified, section area free	σ_e/ρ
Torsion bar or tube. Cyclic torque and length specified, section area free	$\sigma_e^{2/3}/\rho$
Beam. Cyclic bending load or moment and length specified, section area free	$\sigma_e^{2/3}/\rho$
Panel. Cyclic bending load or moment, length and width specified, thickness free	$\sigma_e^{1/2}/\rho$
Panel. Cyclic in-plane tensile load, length and width specified, thickness free	σ_e/ρ
Rotating disks, flywheels. Energy storage specified	σ_e/ρ
Cylinder with internal pressure. Pressure cycle and radius specified; wall thickness free	σ_e/ρ
Spherical shell with internal pressure. Pressure cycle and radius specified; wall thickness free	σ_e/ρ

[a]To minimise *cost*, use the above criteria for minimum weight, replacing density ρ by $C\rho$, where C is the cost per kg. To minimise *energy content*, use the above criteria for minimum weight replacing density ρ by $q\rho$ where q is the energy content per kg.
[b]E = Young's modulus; G = shear modulus; σ_e = endurance limit; ρ = density.

(b) Infinite life design at minimum weight (cost, energy)[a]; precracked samples

Component shape and loading[b]	Crack length fixed Maximise	Crack length = min. section Maximise
Tie (tensile strut). Cyclic load and length specified, section area free	$\Delta K_{th}/\rho$	$\Delta K_{th}^{4/3}/\rho$
Torsion bar or tube. Cyclic torque and length specified, section area free	$\Delta K_{th}^{2/3}/\rho$	$\Delta K_{th}^{4/5}/\rho$
Beam. Cyclic bending load or moment and length specified, section area free	$\Delta K_{th}^{2/3}/\rho$	$\Delta K_{th}^{4/5}/\rho$
Panel. Cyclic bending load or moment, length and width specified, thickness free	$\Delta K_{th}^{1/2}/\rho$	$\Delta K_{th}^{2/3}/\rho$
Panel. Cyclic in-plane tensile load, length and width specified, thickness free	$\Delta K_{th}/\rho$	$\Delta K_{th}^{2}/\rho$
Rotating disks, flywheels. Energy storage specified	$\Delta K_{th}/\rho$	$\Delta K_{th}/\rho$
Cylinder with internal pressure. Pressure cycle and radius specified; wall thickness free	$\Delta K_{th}/\rho$	$\Delta K_{th}^{2}/\rho$
Spherical shell with internal pressure. Pressure cycle and radius specified; wall thickness free	$\Delta K_{th}/(1-\nu)\rho$	$\Delta K_{th}^{2}/(1-\nu)\rho$

[a]To minimise *cost*, use the above criteria for minimum weight, replacing density ρ by $C\rho$, where C is the cost per kg. To minimise *energy content*, use the above criteria for minimum weight replacing density ρ by $q\rho$ where q is the energy content per kg.
[b]ΔK_{th} = threshold stress intensity range; ρ = density; ν = Poisson's ratio.

(c) Infinite life design: springs, hinges, diaphrams etc.

Component and design goal[a]	Maximise
Springs. Cyclically loaded; specified energy storage, volume to be minimised	σ_e^2/E
Springs. Cyclically loaded; specified energy storage, mass to be minimised	$\sigma_e^2/E\rho$
Elastic hinges. Repeated bending; radius of bend to be minimised	σ_e/E
Knife edges, pivots. Cyclically loaded; minimum contact area, maximum bearing load	σ_e^3/E^2 and E
Compression seals and gaskets. Cyclically loaded; maximum contact area with specified maximum contact pressure	σ_e/E and $1/\sigma_e$
Diaphragms. Cyclically loaded; maximum deflection under specified pressure or force	$\sigma_e^{3/2}/E$
Rotating drives, centrifuges. Maximum angular velocity, radius specified, wall thickness free	σ_e/ρ

[a]σ_e = endurance limit; E = Young's modulus; ρ = density.

(d) Damage-tolerant design etc.

Component and design goal[a]	Maximise
Tensile member. Cyclic loading, load-controlled design	ΔK_{th} and σ_e
Tensile member. Cyclic loading, displacementcontrolled design	$\Delta K_{th}/E$ and σ_e/E
Tensile member. Cyclic loading, energy-controlled design	$\Delta K_{th}^2/E$
Pressure vessel. Cyclic loading, yield-before-break	$\Delta K_{th}/\sigma_e$
Pressure vessel. Cyclic loading, leak-before-break	$\Delta K_{th}^2/\sigma_e$
Thermal fatigue resistance. Temperature cycling	$\sigma_e/E\alpha$

[a]σ_e = endurance limit; E = Young's modulus; ΔK_{th} = threshold stress intensity range; α = thermal expansion coefficient.

or mechanical working. These ranges appear as little bubbles on the chart, one bubble enclosing data for one material or sub-class of materials.

The following assumptions have been made in presenting the data. The yield strength, for ductile materials, is the 0.2% offset yield; it is approximately the same in tension and compression. That for ceramics and woods refers to the tensile fracture strength. Data for woods are shown in two groups, one describing properties along the grain, the other, those across the grain. The yield strength of elastomers is the nominal stress at a nominal strain of unity. The data for composites are for polymeric matrix composites with long fibre carbon, Kevlar and glass fibre reinforcement. Properties are given for both multi-directional "quasi-isotropic" laminates, and for unidirectional material in a direction parallel to the fibres.

2. DEFINITIONS AND BACKGROUND

2.1. *The fatigue properties*

First, some definitions. The cyclic stress range $\Delta\sigma$ (Fig. 2) is defined as the difference between the peak σ_{max} and the trough σ_{min} of the stress cycle

$$\Delta\sigma = \sigma_{max} - \sigma_{min}. \tag{1a}$$

The cyclic stress amplitude σ_a is half the stress range

$$\sigma_a = \frac{\sigma_{max} - \sigma_{min}}{2}. \tag{1b}$$

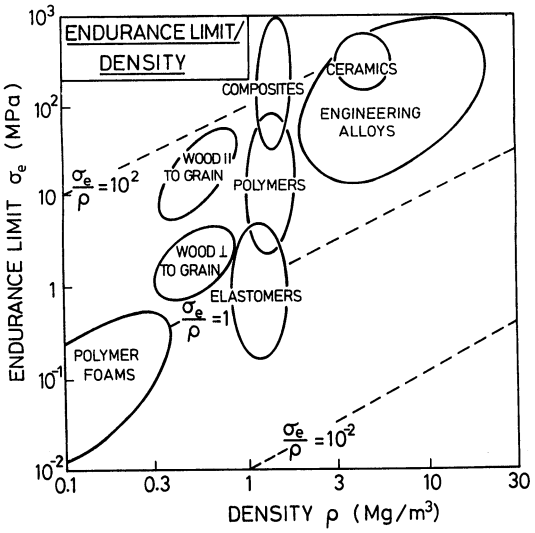

Fig. 1. A schematic of a materials selection chart. The axes, in this example, are the endurance limit σ_e and the density ρ.

The mean stress σ_m is

$$\sigma_m = \frac{\sigma_{max} + \sigma_{min}}{2} \tag{2a}$$

and the load ratio R is commonly used as a measure of the mean stress of the cycle

$$R = \frac{\sigma_{min}}{\sigma_{max}}. \tag{2b}$$

The *endurance or fatigue limit* σ_e is the stress amplitude which a smooth, unnotched sample will sustain without fracture for 10^7 cycles; for many practical purposes 10^7 cycles can be thought of as "infinite" life. Most data derive from tests (such as the rotating-bend test) in which the mean stress is zero and $R = -1$; for this reason the endurance limit is usually quoted for $R = -1$. We follow this convention in presenting values for the endurance limit later in the paper.

A second set of definitions relates to a specimen or structure containing a crack long enough that linear-elastic fracture mechanics applies, that is, the crack is long compared to structural features such as grains. The cyclic mode I stress-intensity, ΔK (Fig. 3), is the difference between the maximum and minimum values of the mode I stress intensity

$$\Delta K = Y(\sigma_{max} - \sigma_{min})\sqrt{\pi a} \tag{3}$$

where a is the current crack length and Y is a non-dimensional geometric factor of order unity, the precise value of which depends upon the geometry of the sample. The *threshold stress intensity range* ΔK_{th} is defined as the value of ΔK below which the crack grows at a rate of less than 10^{-7} mm/cycle. Commonly, ΔK_{th} is quoted for $R = 0$ such that

$$\Delta K_{th} = Y\sigma_{max}\sqrt{\pi a}. \tag{4}$$

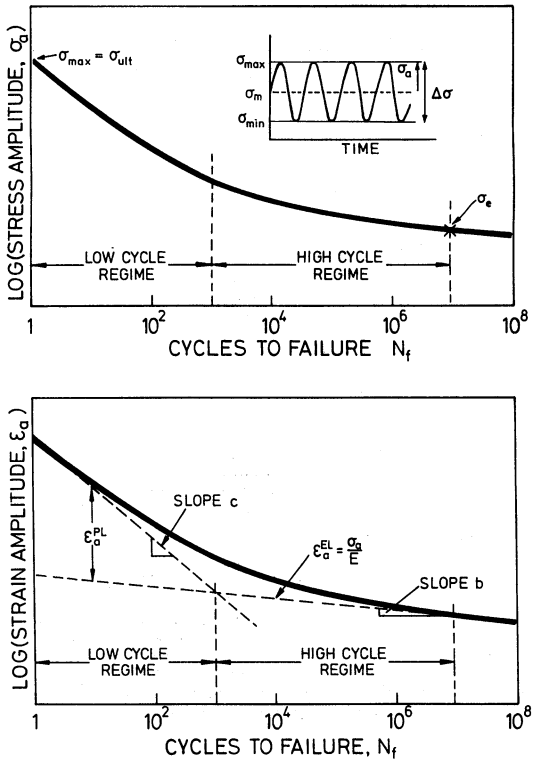

Fig. 2. The σ_a–N_f and the ϵ_a–N_f curves, showing the definitions of cyclic stress amplitude, the endurance limit and the exponents b and c.

Cycling at $R = 0$ generally results in crack closure: the meeting of the faces of the crack so that, for part of the cycle, the stress state at the crack tip is unchanging. When data permit, an adjusted threshold intensity, $(\Delta K_{eff})_{th}$ is reported: it is that portion of ΔK for which the crack is open

$$(\Delta K_{eff})_{th} = Y(\sigma_{max} - \sigma_c)\sqrt{\pi a} \tag{5}$$

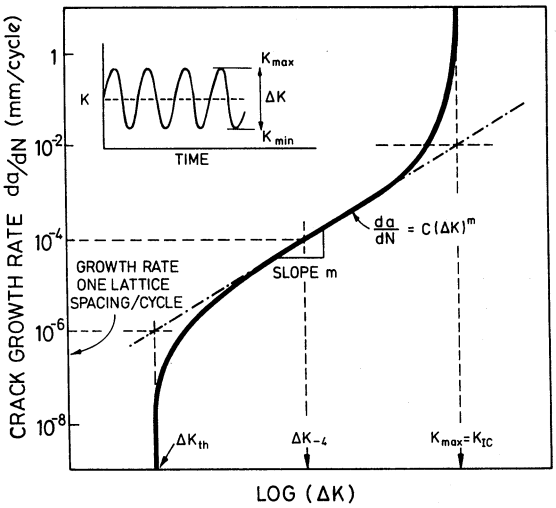

Fig. 3. The da/dN–ΔK curve, showing the definition of cyclic stress intensity, threshold stress intensity, n-value and fracture toughness.

where σ_c is the stress at which the crack closes. The quantity $(\Delta K_{eff})_{th}$ is deduced from crack closure measurements, or is assumed to be equal to ΔK_{th} measured at $R \geqslant 0.8$.

Design for "infinite" fatigue life ($N_f > 10^7$ cycles) requires data for σ_e and ΔK_{th}. But design does not always aim for infinite life. Then further properties, illustrated by Figs 2 and 3, become important.

A phenomenological description of the total fatigue life is given by plotting stress or strain amplitude σ_a or ϵ_a against the number of cycles to failure, N_f (Fig. 2), giving what is known as the S–N curve. It is difficult to model the S–N curve mechanistically because it is the failure envelope resulting from a sequence of interdependent processes: cyclic hardening or softening, crack nucleation and crack growth to final failure. Empirical descriptions date back to the early years of the century (see Ref. [3] for a review). In the "high cycle" regime, a good description is given by

$$\sigma_a = \sigma_f'(2N_f)^b \tag{6}$$

where σ_f' is the fatigue strength coefficient (roughly equal to the fracture strength in tension) and b is the Basquin exponent; it has a value near 0.1 for most metals. Since the sample is almost elastic in this regime the strain amplitude ϵ_a is almost equal to the elastic strain amplitude ϵ_a^{EL}

$$\epsilon_a \approx \epsilon_a^{EL} = \frac{\sigma_f'}{E}(2N_f)^b$$

where E is Young's modulus.

Under larger loads, the sample deforms plastically on each cycle. In this, the "low-cycle" regime, a correlation is found between N_f and the plastic strain amplitude, ϵ_a^{PL}, described by the Coffin–Manson law (3)

$$\epsilon_a^{PL} = \epsilon_f'(2N_f)^c \tag{7}$$

where ϵ_f' is the fatigue ductility coefficient and c is the Coffin exponent (approximately 0.5 for metals). The total strain amplitude is the sum of the elastic and plastic parts, giving

$$\epsilon_a = \frac{\sigma_f'}{E}(2N_f)^b + \epsilon_f'(2N_f)^c. \tag{8}$$

This is illustrated in Fig. 2, which shows the transition from low to high cycle behaviour at

$$2N_f = \left(\frac{\epsilon_f' E}{\sigma_f'}\right)^{1/(c-b)}$$

or typically about 1000 cycles.

When a crack of sufficient length pre-exists, cyclic loading causes it to grow, leading ultimately to failure. The typical crack growth response is illustrated in Fig. 3. The relation between the crack growth rate, da/dN, and ΔK is sigmoidal in shape, the growth rate falling to zero (or, more precisely, to less than 10^{-7} mm/cycle) at the threshold ΔK_{th}. The mid-range, on log scales, is often linear and well described by the empirical equation (3)

$$\frac{da}{dN} = C(\Delta K)^n \tag{9}$$

where C (the crack growth coefficient) and n (the Paris exponent) are constants. In its simplest dimensionally consistent—though not very accurate—form this becomes

$$\frac{da}{dN} = \bar{C}\left(\frac{\Delta K}{E}\right)^2 \tag{10}$$

where $\bar{C}$ is found empirically (4) to have a value of approximately 3. This linear region spans the growth rates from 10^{-5} to 10^{-3} mm/cycle—an important range in design. At higher values of ΔK the crack growth accelerates, becoming catastrophic as K_{max} approaches the fracture toughness K_{Ic}.

A useful construction is added to Fig. 3. If a tangent is drawn at the mid-point of the central linear region of the curve (at about $da/dN = 10^{-4}$ mm/cycle) and extrapolated, it is found empirically that it intersects the line $\Delta K = \Delta K_{th}$ near 10^{-6} mm/cycle, and (for $R = 0$) it intersects the line $\Delta K = K_{Ic}$ at about 10^{-2} mm/cycle. Thus

$$\frac{\log K_{Ic} - \log \Delta K_{th}}{\log(10^{-2}) - \log(10^{-6})} \approx n \tag{11}$$

or

$$\log\left(\frac{\Delta K_{th}}{K_{Ic}}\right) \approx -\frac{4}{n} \tag{12}$$

—a result used later on.

Equations (3) and (9) suggest that the stress amplitude $\sigma_a \equiv (\sigma_{max} - \sigma_{min})/2$ needed to make a pre-existing crack grow increases without bound as the crack length a_0 decreases to zero. In reality the endurance limit sets an upper limit to σ_a. In single crystals this is because cyclic plasticity is capable of producing surface damage with crack-like profiles which are sharper and deeper than the surface undulations produced by high-quality engineering finishes. In polycrystals cracks may nucleate in this way, or may preexist (cracked carbides in steels, for instance); the endurance limit is commonly the stress amplitude required to overcome all barriers to growth (see Section 3.1, below). The regime of incipient crack growth from a pre-existing flaw is distinguished from that of self-organised crack nucleation and growth in Fig. 4; together, they define the $\sigma_a - a_0$ domain in which life, for practical purposes, is infinite.

3. MICROSCOPIC INTERPRETATIONS OF ENDURANCE LIMIT AND FATIGUE THRESHOLD

At the microscopic level, a partial understanding of fatigue damage now exists.

3.1. The endurance limit and the S–N curve

In metals, cyclic straining above a critical plastic-strain amplitude is accompanied by localised bands

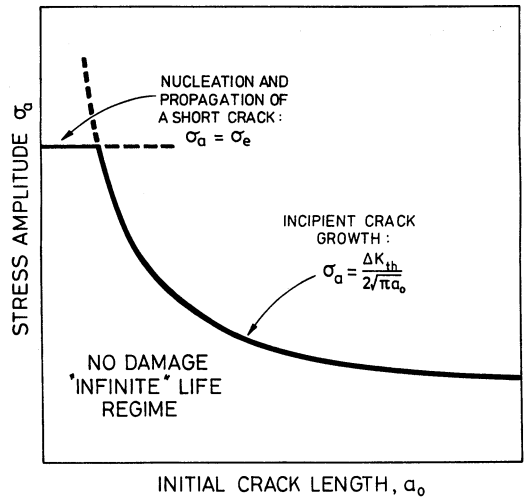

Fig. 4. The endurance limit σ_e and the stress amplitude for long crack growth, plotted against crack length.

of intense slip producing surface roughness which deepens into cracks. Optical microscopy [5] establishes their persistence, even when the surface is repolished; electron microscopy [6–11] shows that the bands are internally stressed and have a unique, planar, dislocation structure; and scanning tunnelling microscopy [12, 13] reveals that the surface damage grows because a small fraction of the slip within a band is irreversible (that is, slip on the tensile half-cycle is not exactly reversed on the compressive half cycle); cracks appear and grow only after a "nucleation" period during which the unique dislocation structure and pattern of internal stress develops.

It has been suggested [7, 11] that a true endurance-limit and a corresponding strain-limit (connected through the cyclic stress–strain curve) exist for crystalline materials. For single crystals they are the limits for the stress and strain below which persistent slips bands do not form. For polycrystals and polyphase metals, the endurance limit is, frequently, the stress amplitude below which cracks do not propagate, rather than a crack nucleation limit [14, 15]. For these, persistent slip bands can develop in individual surface grains at stress amplitudes *below* the endurance limit, but the cracks nucleated in this way do not always propagate. Below the endurance limit, the cracks arrest when they approach an obstacle such as a grain boundary or a second phase particle. Above the endurance limit, the stress intensity at the cracks is sufficiently high for at least one of them to overcome all local barriers and become a dominant macroscopic mode I crack. This macro-crack then grows across the sample and causes failure.

For ceramics, the endurance limit is the stress amplitude at which an existing crack propagates across the sample. This stress is almost the same as the static failure stress, and for this reason the fatigue ratio for most ceramics is about unity. The mechanism of fatigue in non-crystalline solids such as polymers is not clearly understood. Most polymers appear to undergo cyclic softening by progressive molecular disentanglement. The endurance limit is associated with the critical stress amplitude required to nucleate a craze or a crack; once a crack has nucleated there is no further barrier to crack propagation and failure ensues [16].

Given the need for slip, it is not surprising that the endurance limit, for a given class of materials, is proportional to the yield strength (Section 4.1, below). The full microscopic model for the shape of the S–N curve is more difficult, for the reason given earlier. It is the failure envelope associated with a sequence of interdependent phenomena: cyclic hardening, crack nucleation and cyclic growth, and final fast fracture.

3.2. The fatigue threshold and the da/dN–ΔK curve

The fatigue threshold, like the endurance limit, characterises a loading state below which no damage accumulates in the material, but now attention focuses on the crack-tip region rather than the bulk. There have been a number of attempts to give a microscopic interpretation for ΔK_{th}. In a purely elastic system, the elastic energy released at the peak of a cycle must at least be sufficient to create two new surfaces, each with an energy per unit area of γ. It follows that a necessary, though not always sufficient, condition for fatigue-crack growth is that K_I at the peak of the cycle gives an energy release rate of at least 2γ, leading to the "Griffith's" condition

$$\Delta K_{th} \geqslant (2\gamma E)^{1/2}. \tag{13}$$

The surface energies of solids scale as their moduli; as a rule of thumb

$$\gamma = \frac{Er_0}{20}$$

where r_0 is the atom size, giving

$$\Delta K_{th} \geqslant E\left(\frac{r_0}{10}\right)^{1/2}. \tag{14}$$

Taking r_0 as 1 to 3×10^{-10} m, we find

$$3 \times 10^{-6}\,\mathrm{m}^{1/2} \leqslant \frac{\Delta K_{th}}{E} \leqslant 5 \times 10^{-6}\,\mathrm{m}^{1/2}. \tag{15}$$

An alternative argument giving much the same result is to associate the threshold with the attainment of a critical cyclic crack-tip opening Δv at one atomic spacing (r_0) behind the crack tip. The elastic solution for a loaded crack tip gives

$$\Delta v = \frac{\Delta K_{th}\sqrt{r_0}}{3E}. \tag{16}$$

We assume that the crack ceases to grow if $\Delta v < 0.1\, r_0$, since this, roughly speaking, is the failure extension of an atomic bond, giving (for the same limits for r_0)

$$2 \times 10^{-6}\,\mathrm{m}^{1/2} \leqslant \frac{\Delta K_{th}}{E} \leqslant 4 \times 10^{-6}\,\mathrm{m}^{1/2}. \tag{17}$$

Yet another estimate is found by postulating that, at ΔK_{th}, the crack growth rate has fallen to less than one atom spacing per cycle [4, 11]. This implies via the approximate equation (10)

$$7 \times 10^{-6}\,\mathrm{m}^{1/2} \leqslant \frac{\Delta K_{th}}{E} \leqslant 10^{-5}\,\mathrm{m}^{1/2}.$$

But despite the consistency of these estimates, the models, while perhaps realistic for fatigue under vacuum with no anelastic heating, are incomplete; they do not, for instance, explain the established dependence of ΔK_{th} on the environment in which the test is carried out.

Elastomers and many polymers have thresholds which lie at a larger fraction of E because of the low moduli associated with their weak van der Waals bonding and because the crack tip in these materials is blunted, stretching open to a distance of the order of the adjacent cross-links of the polymer chain structure [17]. If the crack is to propagate, molecular segments with lengths up to the cross-link spacing span the crack tip. These must be stretched to failure as the crack propagates. It is not one bond (length r_0) that is being stretched to failure (failure displacement $0.1\,r_0$) but rather a chain of length, perhaps, $100\,r_0$, giving a displacement of $10\,r_0$ and [via equation (16)] a threshold which is an order of magnitude greater than that of equation (17).

Microscopic models for the shape of the da/dN–ΔK curve (3) seek to explain the slope of the linear, central region. The underlying postulate is that the crack advance per cycle is proportional to the size of the process or plastic zone at the crack tip, leading to the growth law

$$\frac{da}{dN} = C\left(\frac{\Delta K}{\sigma_{cy}}\right)^2 \qquad (18)$$

where C is a constant. The cyclic yield strength, σ_{cy}, is proportional to the yield strength, σ_y, suggesting a quadratic dependence of da/dN on $\Delta K/\sigma_y$. In practice this appears to be a lower limit for the slope—it is usually steeper (typically 4 rather than 2). Current models do not fully explain this.

4. FATIGUE PROPERTY CHARTS: DESIGN FOR INFINITE LIFE

The following sections describe charts which relate fatigue properties to static properties and to each other. They reveal correlations for which, in some cases, microscopic models exist; and they provide a method of selecting materials for mechanical design.

4.1. The endurance limit—yield strength chart (Fig. 5)

Figure 5 shows the well-known fact that the endurance limit σ_e scales in a roughly linear way with the yield strength, σ_y. The *fatigue ratio*, defined as σ_e/σ_y at $R = -1$, appears as a set of diagonal contours. Its value, for engineering materials, usually lies between 0.3 and 1. Generally speaking, it is near 1 for monolithic ceramics, about 0.5 for metals and elastomers, and about 0.3 for polymers, foams and wood; the values for composites vary more widely—from 0.1 to 0.5. There are some exceptions: the fatigue ratio of annealed copper can be as high as 2.5 because of work hardening; that for certain peak aged aluminium alloys can be as low as 0.2 because of cyclic softening.

Cracks either do not initiate or are unable to propagate at stress amplitudes below the endurance limit. Below this limit, deformation within the bulk of the material is elastic (that is, completely reversible) or anelastic (with some anelastic energy dissipation but not accumulation of damage). When this is so, one expects a correlation of σ_e with σ_y or with the ultimate strength σ_{ult}, provided, of course, that no stress concentrations or cracks are present in the sample, and that it is internally homogeneous. Stress concentrations, or modulus differences between phases, elastic anisotropy between grains, or brittle grain boundary layers will upset the correlation by introducing sites of local plasticity or cracking, and thus damage. The figure shows that relatively pure, soft metals have a fatigue ratio near 1; fully hardened steels (in which there is the potential for the nucleation of a brittle crack) and fully hardened aluminium alloys (with the capacity for work softening and thus localisation of slip) have lower fatigue ratios, as do some metal–matrix composites. That for polymers is complicated by adiabatic heating; rapid cycling, even in the nominally elastic range, induces a temperature rise and a consequent loss of strength. The wide range of fatigue ratios shown by composites relates, in part, to the wide spectrum of materials used to make them, and to the necessarily broad definition of failure: in particulate composites, failure means fracture; in fibrous composites it means major loss of stiffness. The exceptionally low endurance limits of many polymeric foams relates to the early propagation of the incipient cracks they contain.

As a general rule, initially soft metals and alloys show cyclic hardening and a large fatigue ratio ($\sigma_e > \sigma_y$); metals and alloys which are initially heavily work-hardened or hardened by precipitates tend to cyclically soften and have low fatigue ratios ($\sigma_e < \sigma_y$). This is illustrated by Fig. 6. It shows the fatigue ratio for metallic alloys plotted against the yield strength σ_y on logarithmic scales. The figure suggests that

$$\frac{\sigma_e}{\sigma_y} \propto \sigma_y^{-m}$$

with $0.3 < m < 0.5$ and accounts for the slopes of the bubbles in Fig. 5.

The relationship between endurance limit σ_e, yield strength σ_y and cyclic yield strength σ_{cy} is shown in Fig. 7(a) for steels and in Fig. 7(b) for aluminium alloys, this time on linear scales. Conventionally, the cyclic yield strength σ_{cy} is defined as the 0.2% proof stress of the cyclic stress–strain curve (at half life of

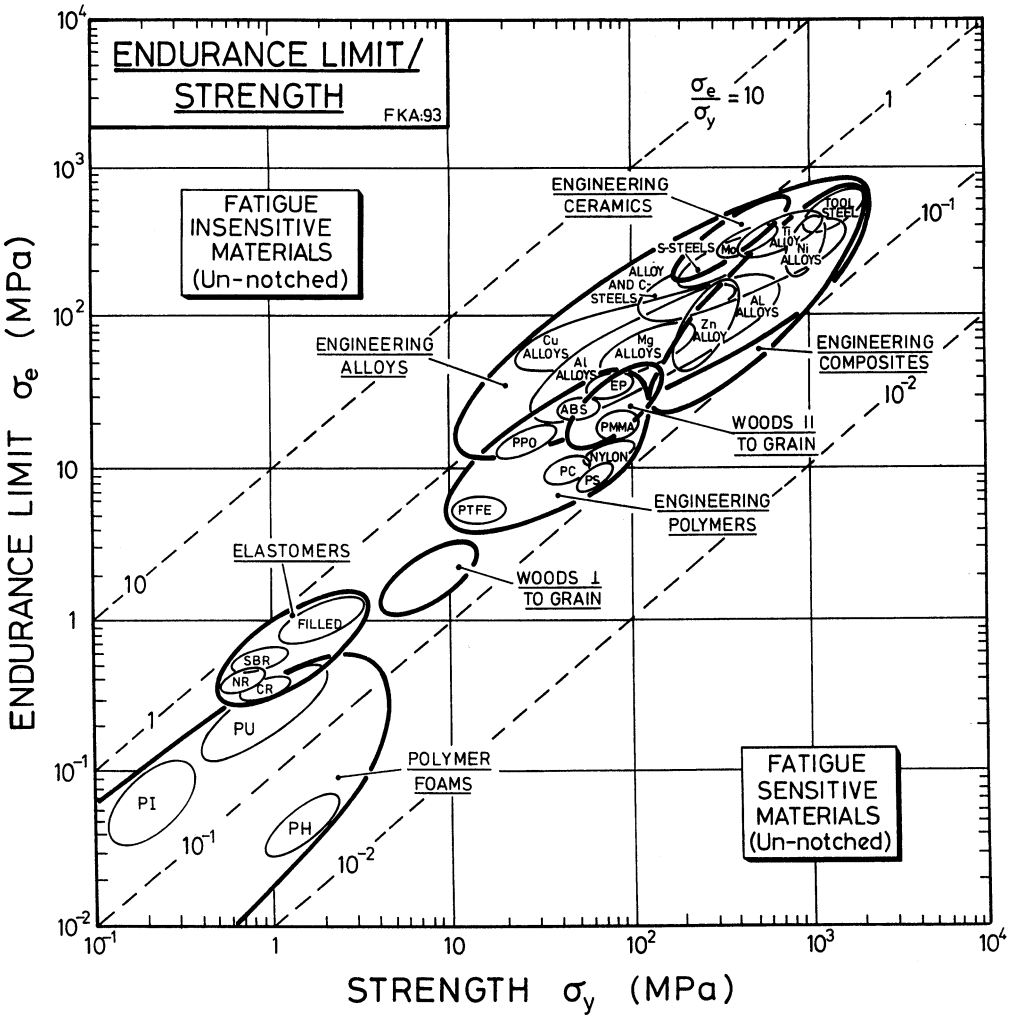

Fig. 5. The endurance limit σ_e (at a load ratio $R = -1$) vs yield strength σ_y.

the unnotched specimen). It is seen that at low values of yield strength (below about 1000 MPa for steels and about 200 MPa for aluminium alloys) σ_e is approximately equal to σ_{cy}. At higher values of σ_y the endurance limit σ_e lies in the range 500–700 MPa for steels and 150–250 MPa for aluminium alloys. The cyclic strain amplitudes at the endurance limit are in the range 0.2% and 0.35% for both materials. These deductions support the notion that the cyclic yield stress is a bulk measure of the stress for plastic flow throughout the solid; it scales with the monotonic yield stress in a roughly linear manner. The endurance limit, on the other hand, is the strength of the "weakest link" within the solid, and increases only slowly with increasing bulk strength.

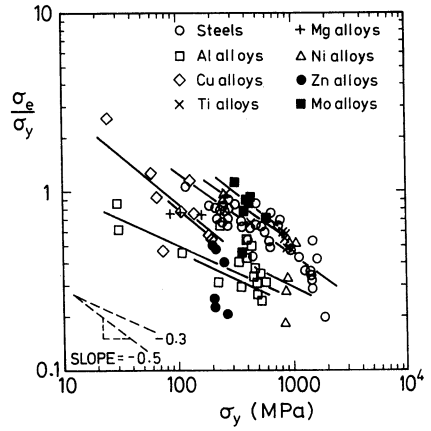

Fig. 6. The fatigue ratio σ_e/σ_y plotted against the yield strength σ_y of metallic alloys.

The endurance limit depends on the mean stress σ_m [equation (2a)] of the fatigue cycle. For ductile metals the dependence is less strong than that for brittle solids such as ceramics. Data for the influence of the mean stress upon the endurance limit of metals are shown in Fig. 8. The data are adequately represented by the expression

$$\frac{(\sigma_e)_{\sigma_m}}{\sigma_y} + 0.4\frac{\sigma_m}{\sigma_y} = 1. \tag{19}$$

Here σ_e is the endurance limit at $\sigma_m = 0$ and $(\sigma_e)_{\sigma_m}$ is that at a non-zero mean stress σ_m. Assuming a typical value of 0.5 for the fatigue ratio of metals, this implies

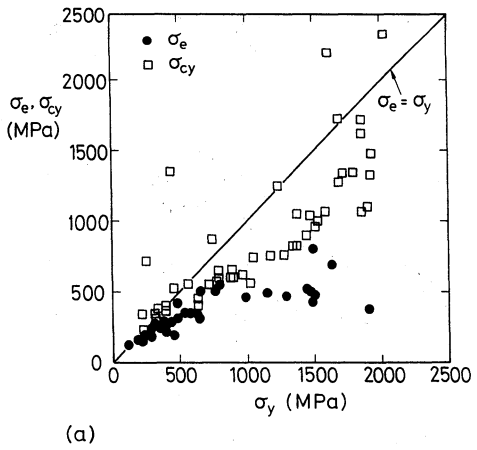

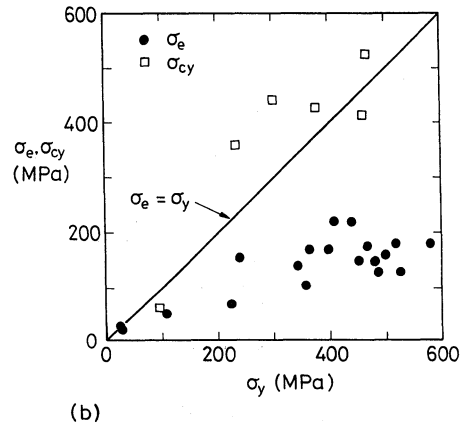

Fig. 7. The endurance limit σ_e and cyclic yield stress σ_{cy} plotted against yield strength σ_y, for (a) steels and (b) aluminium alloys.

that the endurance limit at $R = 0$ is approximately 10% less than the endurance limit at $R = -1$. For ceramics fatigue failure occurs when the maximum stress in the fatigue cycle equals the static failure strength, implying that, for these materials

$$\frac{(\sigma_e)_{\sigma_m}}{\sigma_y} + \frac{\sigma_m}{\sigma_y} = 1. \tag{20}$$

Elastic design requires that the component or structure remains in the elastic regime throughout service. In selecting materials to withstand static loads, it is adequate to base the design on the yield strength, reduced by a suitable safety factor. Since the fatigue ratio varies by a factor of 5 or more, materials selection for cyclic loads should be based, instead, on the endurance limit. Then the performance indices for various aspects of fatigue limited design, listed in Table 1, should be used.

†For the toughened ceramics, we use the symbol K_{Ic} to denote the steady state toughness rather than the initiation toughness.

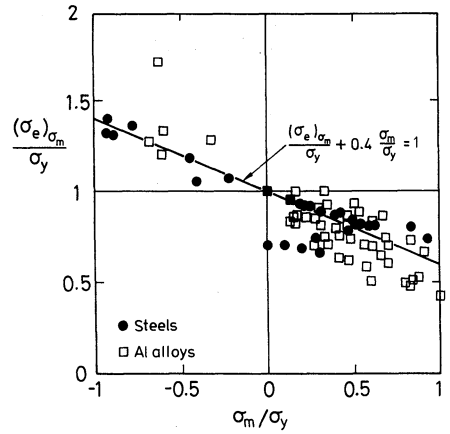

Fig. 8. The endurance limit $(\sigma_e)_{\sigma_m}$ plotted against the mean stress σ_m of the fatigue cycle. Both axes are normalised with respect to the yield stress σ_y.

4.2. The fatigue threshold–fracture toughness chart (Fig. 9)

The fatigue threshold ΔK_{th} is plotted against the fracture toughness K_{Ic} in Fig. 9. Diagonal contours show the ratio $\Delta K_{th}/K_{Ic}$. It ranges from 0.03 for tough steels and titanium alloys to 0.8 for certain polymers and ceramics, although that for most materials lies in the narrower range from 0.05 to 0.5. One might expect a correlation between ΔK_{th} and K_{Ic}, and on the broadest scale, this is found (see Fig. 9). But within a given material class, the correlation is much less good than that of σ_e with σ_y. In general, the ratio $\Delta K_{th}/K_{Ic}$ is lower than the ratio σ_e/σ_y; in this sense, cracked materials are more sensitive to fatigue loading than those which are initially uncracked. Polymers and woods are the exception; for these materials it seems that the two ratios are about equal. Fibrous composites do not appear in Fig. 9 because they do not fail in fatigue by single-crack propagation.

From a design standpoint, little is gained in designing against fatigue when $\Delta K_{th}/K_{Ic}$ is greater than, say, 0.7 unless the load range (and thus ΔK) is very accurately known. Design based on K_{Ic} alone is adequate; it is for this reason that monotonic design considerations suffice for many polymers and ceramics. However, it is found that material developments to improve K_{Ic} generally result in a reduced ratio of $\Delta K_{th}/K_{Ic}$—that is, they make the material more sensitive to fatigue, suggesting behaviour which parallels that for the fatigue ratio shown in Fig. 6. Dauskardt *et al.* [18], for example, observe that mechanisms which toughen ceramics under monotonic loading are much less effective in fatigue: transformation toughening becomes less potent, and crack bridging mechanisms are of less benefit because the bridging ligaments suffer low cycle fatigue failure behind the main crack tip. Thus the ratio $\Delta K_{th}/K_{Ic}$ for *toughened* ceramics can be small, and design against fatigue becomes important†.

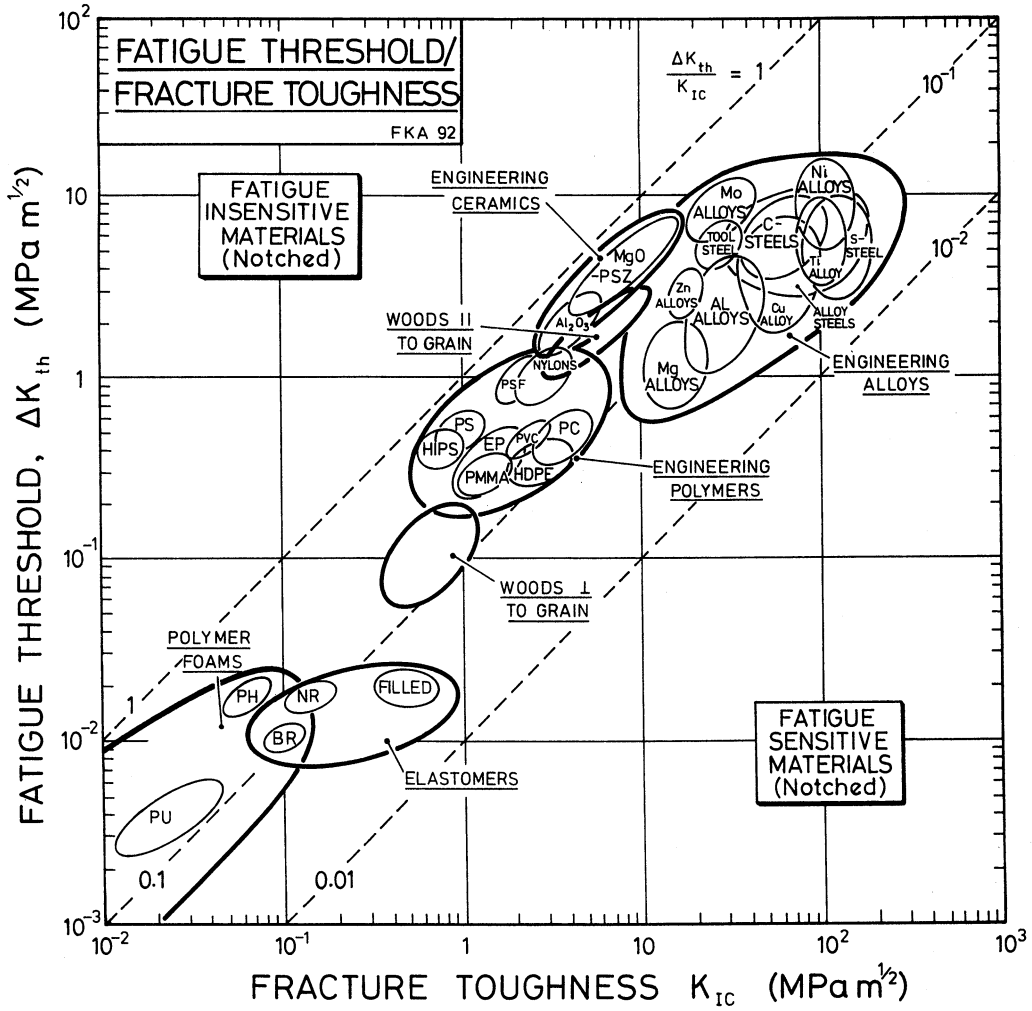

Fig. 9. The threshold stress intensity range ΔK_{th} (at a load ratio $R = 0$) vs fracture toughness K_{Ic}.

4.3. The fatigue threshold–endurance limit chart (Fig. 10)

The fatigue threshold-endurance limit chart of Fig. 10 is the analogue for fatigue of the fracture toughness-yield stress chart shown as Fig. 10 of Ref. [1]. The process zone at a crack tip under cyclic loading of threshold magnitude has diameter

$$d_{cy} \approx \frac{1}{\pi}\left(\frac{\Delta K_{th}}{2\sigma_e}\right)^2 \tag{21}$$

where it is assumed that $\sigma_e \approx \sigma_{cy}$. This, for metals, is the familiar expression for the cyclic plastic zone size. The contours on Fig. 10 show that d_{cy} lies between 10^{-3} and 1 mm for most engineering materials, values which are significantly smaller than the plastic zone size at failure under monotonic loading

$$d_{pl} \approx \frac{1}{\pi}\left(\frac{K_{Ic}}{\sigma_y}\right)^2.$$

We define a transition crack size for fatigue loading in similar manner to that for monotonic loading. Suppose a structure contains a surface crack of length a_0 and is subjected to fatigue loading with $R = 0$. The crack will grow by fatigue provided the local stress amplitude σ_a exceeds the threshold value σ_{th}, where

$$\sigma_{th} = \frac{\Delta K_{th}}{2\sqrt{\pi a_0}}. \tag{22}$$

For sufficiently small crack lengths σ_{th} exceeds σ_e and life is determined by the endurance limit, not the fatigue threshold (Fig. 4). On equating the expression for σ_{th} with σ_e, the transition crack size a_{cy} for infinite fatigue life is found

$$a_{cy} = d_{cy} = \frac{(\Delta K_{th})^2}{\pi(2\sigma_e)^2}. \tag{23}$$

We may interpret a_{cy} as the crack length at which linear-elastic concepts fail and "short crack effects" become important, as first noted by Smith [14] and confirmed experimentally, for metals, by Kitakawa and Takahashi [19].

The bottom right portion of Fig. 10 contains the regime in which fatigue crack growth governs the design of engineering structures (small values of

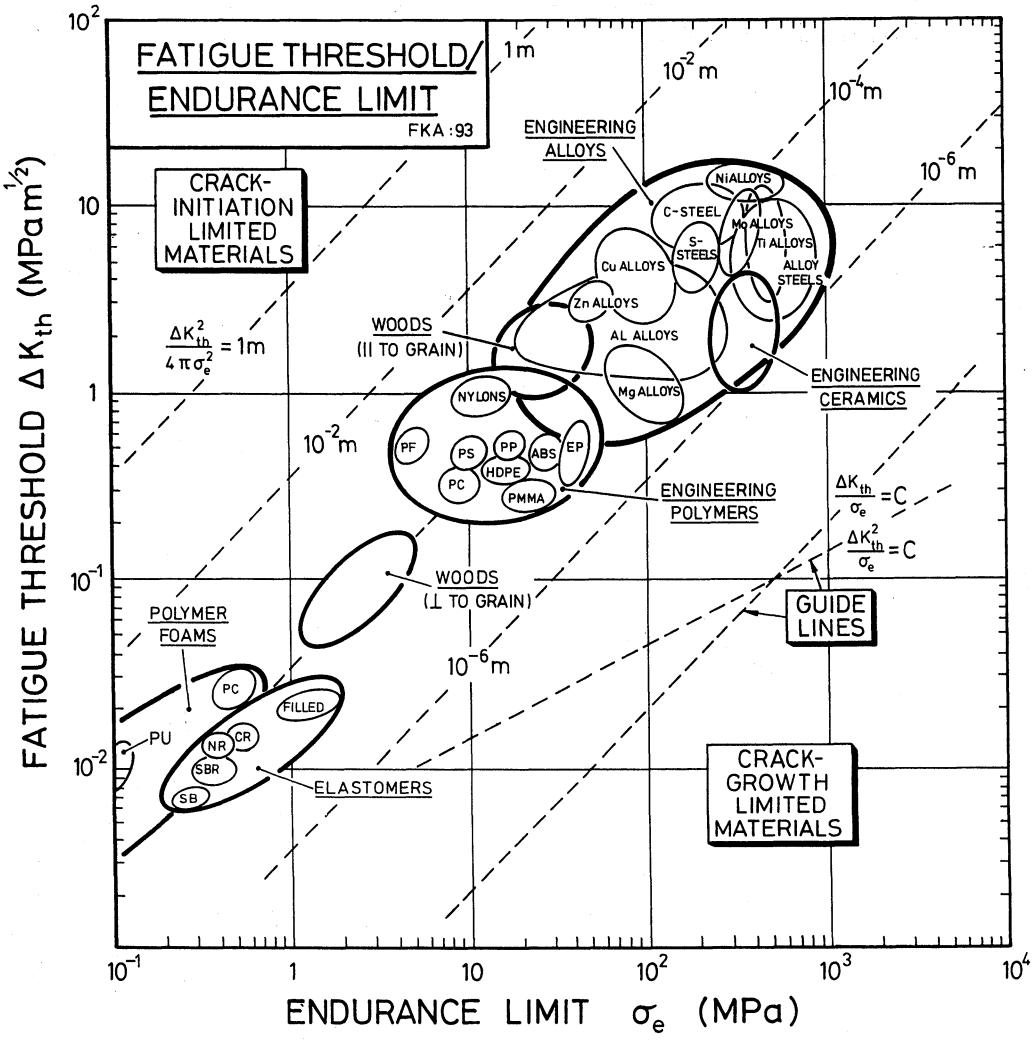

Fig. 10. The threshold stress intensity range ΔK_{th} (at a load ratio $R = 0$) vs endurance limit σ_e (at a load ratio $R = -1$). The contours show the value of $(\Delta K_{th})^2/\pi(2\sigma_e)^2$ which is approximately equal to the diameter of the cyclic process zone at the crack tip (units are m).

$\Delta K_{th}/\sigma_e$), while the top left portion of the chart contains the regime in which considerations of crack initiation become important (large values of $\Delta K_{th}/\sigma_e$). Materials with large values of the performance index $\Delta K_{th}/\sigma_e$ (Table 1) are *crack tolerant*, that is, they can contain relatively long cracks safely at a given fraction of the endurance limit. Materials with small values of $\Delta K_{th}/\sigma_e$ are *crack sensitive*, meaning that their fatigue life is reduced by the presence of a relatively short crack. A guide-line of $\Delta K_{th}/\sigma_e$ is included in Fig. 10. Steels, copper alloys and nickel alloys have the highest values, recommending them for safety-critical applications (pressure vessels, landing gear).

4.4. The fatigue limit–modulus chart (Fig. 11)

The chart of σ_e plotted against E (Fig. 11) suggests that the two are correlated, but the correlation is less good than that of σ_e with σ_y (Fig. 5), and just reflects the fact that E and σ_y themselves are correlated. The chart is, nonetheless, useful. The contours show the fatigue-limit elastic strain-amplitude ϵ_e

$$\epsilon_e = \frac{\sigma_e}{E}$$

which is the analog, for fatigue loading, of the yield strain, $\epsilon_y = \sigma_y/E$. The values of ϵ_e are less than the yield strain by a factor equal to the fatigue ratio, σ_e/σ_y. Typically, $\epsilon_e \approx 0.1$–1 for elastomers, $\epsilon_e \approx 10^{-2}$ for polymers, composites, woods and polymer foams, and $\epsilon_e \approx 3 \times 10^{-3}$ for engineering alloys and ceramics.

Three guide lines are marked on the chart; they correspond to the performance indices σ_e^2/E, $\sigma_e^{3/2}/E$; and σ_e/E. Their uses, summarised in Table 1, are in selecting materials for various sorts of elastic design. Their derivations and applications can be found in Ref. [2].

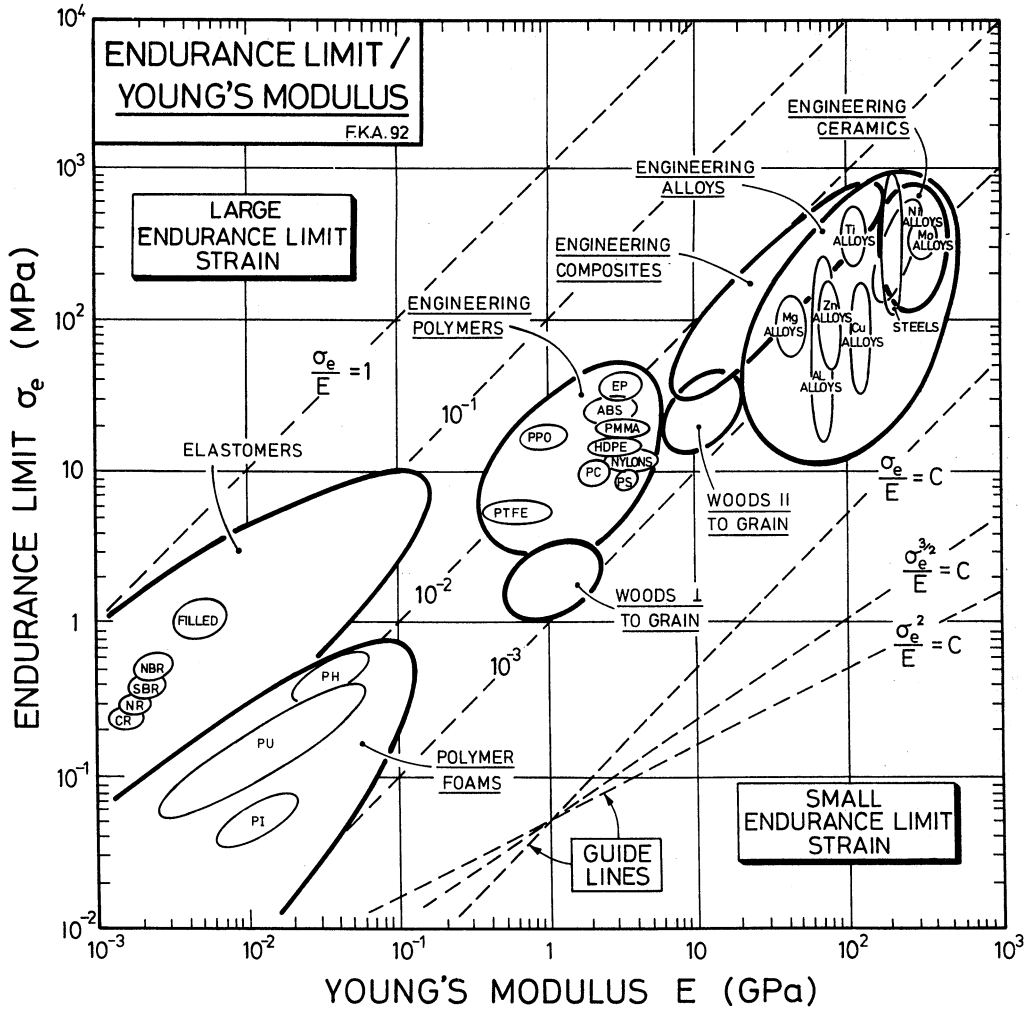

Fig. 11. Endurance limit σ_e (at a load ratio $R = -1$) vs Young's modulus E. The guide line of constant σ_e^2/E helps with the selection of materials for springs; that for constant σ_e/E guides in the selection of materials for elastic hinges.

4.5. The fatigue threshold–modulus chart (Fig. 12)

The microscopic interpretation for ΔK_{th} summarised in Section 3 suggested a correlation between ΔK_{th} and modulus, E. The two are plotted in Fig. 12, to which the lower limit for ΔK_{th} given by equation (15) has been added. Metals and ceramics have thresholds ΔK_{th} which are 3 to 10 times the theoretical limit. Elastomers and many polymers have thresholds which lie at a larger multiple of the limit because of crack blunting (Section 3).

A number of *guide lines for material selection* are plotted on the figure. Consider a cyclically loaded component which contains a crack of length a. The maximum stress range $\Delta\sigma$ which the cross-section can support without failure is approximately $\Delta K_{th}/\sqrt{\pi a}$. For a given load range, the section is minimised by selecting the material with the largest value of ΔK_{th}; steels excell here. Similarly, the maximum strain amplitude which a component can sustain without failure is related to the index $\Delta K_{th}/E$; here polymers, elastomers and foams are good. Finally, in the design of springs and energy-absorbing components of minimum volume performance is maximised by maximising the index $\Delta K_{th}^2/E$; for these, elastomers are good (Table 1).

The value of ΔK_{th} is influenced by crack closure. At high values of the load ratio R (greater than about 0.8) fatigue cracks remain open during the whole of the load cycle and a true fatigue threshold is reached: it is called the "effective threshold", $(\Delta K_{eff})_{th}$. Data for $(\Delta K_{eff})_{th}$ are limited. We have plotted them in the same way as those for ΔK_{th} shown in Fig. 12, but do not show the figure here since it adds little. The data for $(\Delta K_{eff})_{th}$ lie a little lower than those for ΔK_{th} but the ranking of materials remains the same. The Griffith energetic condition for fatigue crack growth, equation (15), should be properly considered in terms of $(\Delta K_{eff})_{th}$ rather than in terms of ΔK_{th}. The correlation between $(\Delta K_{eff})_{th}$ and $E\sqrt{r_0}$ is examined in

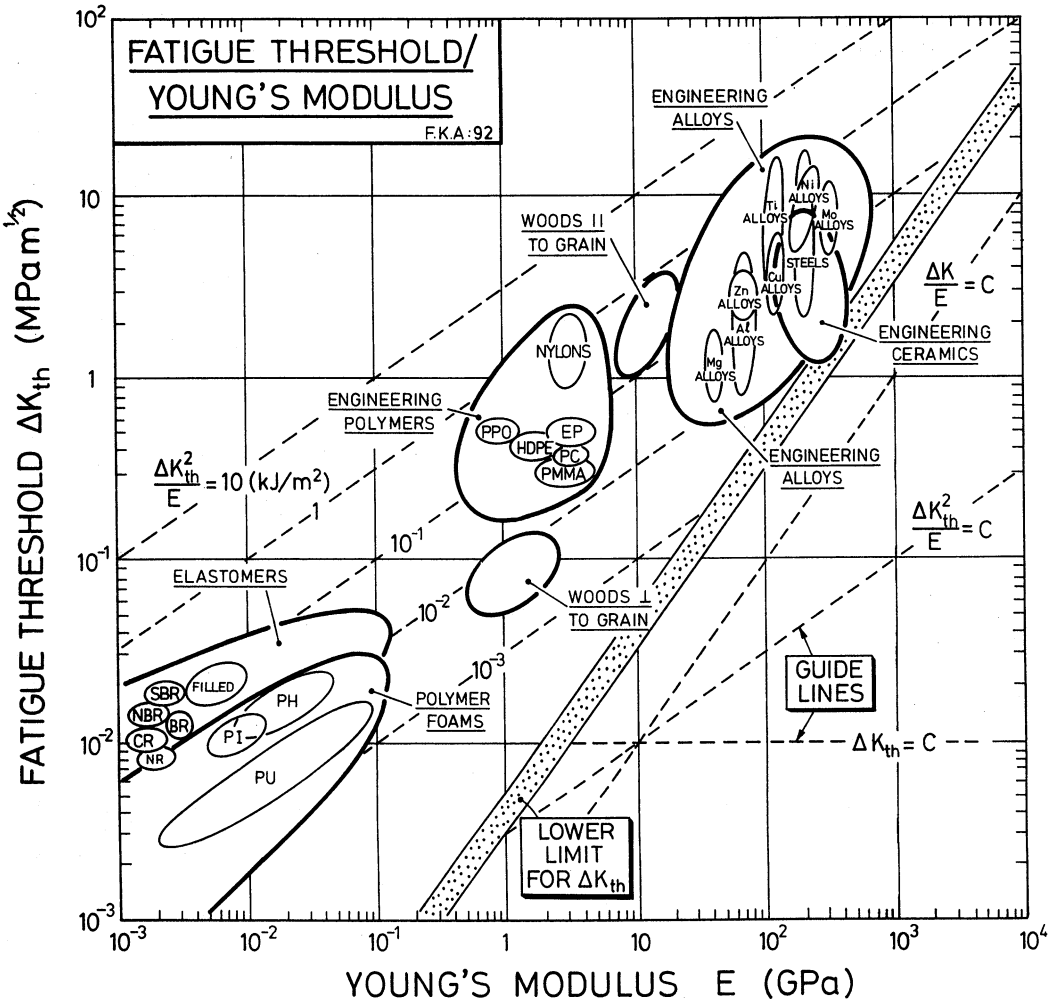

Fig. 12. The threshold stress intensity range ΔK_{th} (at a load ratio $R = 0$) vs Young's modulus E. The chart is useful for deflection-limited design of flawed components. The guidelines ΔK_{th}, $\Delta K_{th}/E$ and $\Delta K_{th}^2/E$ are for load-limited design, deflection-limited design and energy-limited design.

Fig. 13 for a range of metallic alloys, where r_0 is the atom spacing, as before. We find that

$$(\Delta K_{eff})_{th} \approx 1.15E\sqrt{r_0}$$

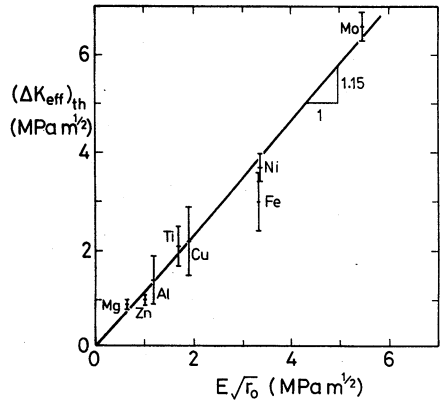

Fig. 13. The effective stress intensity threshold $(\Delta K_{eff})_{th}$ plotted against $E\sqrt{r_0}$ for metallic alloys, where E is Young's modulus and r_0 is the atomic spacing in the close-packed direction.

implying that the measured values of $(\Delta K_{eff})_{th}$ are about 3 times the Griffith's limit for metals.

4.6. The endurance limit, σ_e (at load ratio $R = -1$) —density ρ chart (Fig. 14)

A common design goal is that of achieving infinite fatigue life at minimum weight. Two sets of performance indices are important here. The first set has the form σ_e^n/ρ where n takes values between 0.5 and 1, depending on the mode of loading (Table 1).

The chart of Fig. 14 allows material selection based on maximising these indices. The guide lines of σ_e/ρ, $\sigma_e^{2/3}/\rho$ and $\sigma_e^{1/2}/\rho$ parallel those for yield-limited design under monotonic loads (Ref. [1], Fig. 6). There is some shifting of the relative performance of the various classes of materials relative to that for static loading. Ceramics, for example, have a high fatigue ratio and compete successfully with metals in minimum weight design under fatigue conditions.

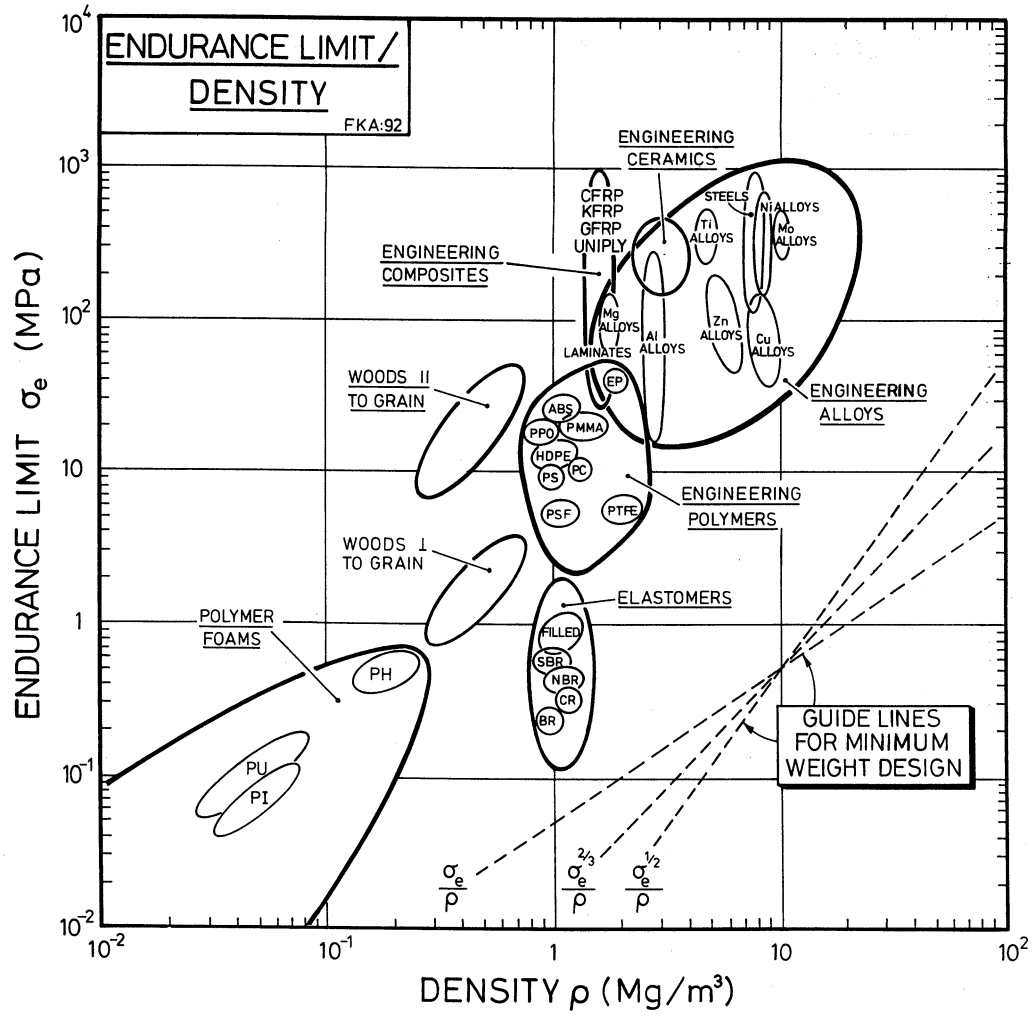

Fig. 14. The endurance limit σ_e (at a load ratio $R = -1$) vs density ρ. The guide lines help in selecting material for light, fatigue-resistant structures.

4.7. The threshold stress intensity range, ΔK_{th} (at load ratio $R = 0$)—density ρ chart, (Fig. 15)

The second set of indices for minimum-weight design takes the form $\Delta K_{th}^n/\rho$ where, again, n takes values between 0.5 and 1; they are the parallel of a set, of form K_{Ic}^n/ρ, for static loading. The chart of Fig. 15 allows selection by these criteria; it serves the same purpose as that of Fig. 14, but for components that contain cracks. The guide lines of $\Delta K_{th}/\rho$, $\Delta K_{th}^{2/3}/\rho$ and $\Delta K_{th}^{1/2}/\rho$ parallel those for static fracture-limited design. A comparison of this chart with the K_{Ic} vs ρ chart given by (Ref. [1], Fig. 7) shows that the crack growth-resistance of metals degrades in fatigue much more than that of other materials. Under cyclic loading, ceramics and woods are good choices for minimum weight design.

5. FATIGUE PROPERTY CHARTS: DESIGN FOR FINITE LIFE

The ability to predict life—even when a crack is growing—is an essential part of efficient design against fatigue. We now turn to design for finite life.

5.1. Paris law index n–$\Delta K_{th}/K_{Ic}$ chart (Fig. 16)

Crack growth during cyclic loading is characterised by the Paris curve shown in Fig. 3. The curve, when plotted on log axes, is sigmoidal in shape with the limits $\Delta K = \Delta K_{th}$ at $da/dN = 10^{-7}$ mm/cycle, and $\Delta K = (1 - R)\,\Delta K_{Ic}$ at $da/dN = 1$ mm/cycle. It is often linear over the range $10^{-5} < da/dN < 10^{-3}$ mm/cycle. It is here that crack growth is described by the Paris law, which we now write as

$$\frac{da}{dN} = C'\left(\frac{\Delta K}{\Delta K_{-4}}\right)^n \text{ mm/cycle} \qquad (24)$$

where ΔK_{-4} is the stress intensity range corresponding to a crack growth rate of $C' \equiv 10^{-4}$ mm/cycle. We interpret equation (24) as the tangent to the $\log(da/dN)$ vs $\log(\Delta K)$ curve at a crack growth rate of 10^{-4} mm/cycle; the exponent n is the slope of this tangent. As explained in Section 2, this leads to the

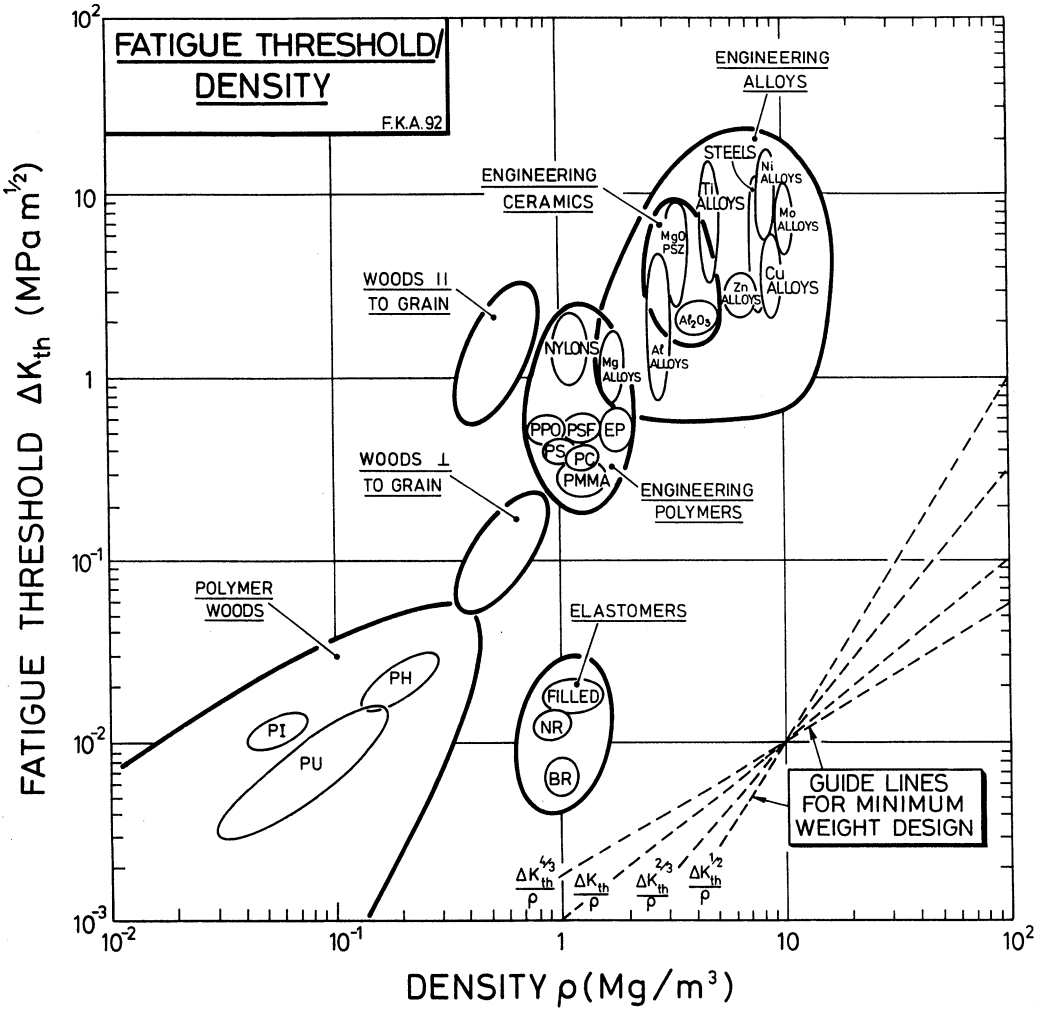

Fig. 15. The threshold stress intensity range ΔK_{th} (at a load ratio $R = 0$) vs density ρ. The guide lines help in selecting material for light, fatigue-resistant structures.

prediction of a linear relationship between $\log(\Delta K_{th}/K_{Ic})$ and the reciprocal of the Paris slope, $1/n$ [equation (12)].

The reciprocal of the Paris exponent, $1/n$, is plotted against $\log(\Delta K_{th}/K_{Ic})$ in Fig. 16, with equation (12) superimposed. The approximately linear correlation is apparent: the Paris index n is necessarily large for materials for which the ratio $\Delta K_{th}/K_{Ic}$ is large.

Taking logs of equation (24) gives

$$\log\left(\frac{da}{dN}\right) = -4 + n \log\left(\frac{\Delta K}{\Delta K_{-4}}\right)$$

where the units of crack growth rate da/dN are mm/cycle. Writing

$$\Delta K_{-4} = (K_{Ic}\,\Delta K_{th})^{1/2} \tag{25}$$

gives, when combined with equation (12), the useful approximation

$$\log\left(\frac{da}{dN}\right) = -2 + n \log\left(\frac{\Delta K}{K_{Ic}}\right). \tag{26}$$

We note from Fig. 16 that metals (particularly medium strength steels and pressure vessel steels) have low values of n and thus of the ratio $\Delta K_{th}/K_{Ic}$; for these, finite life design is practical and cost-effective. Many ceramics and polymers have high values of the index n and values of $\Delta K_{th}/K_{Ic}$ near 1; for these, uncertainties in the loading imply that there is little point in attempting to design for finite fatigue life; design based on the fracture toughness alone suffices.

5.2. *Paris law slope n–ΔK_{-4} chart (Fig. 17)*

Taking $\Delta K \approx \Delta\sigma\sqrt{\pi a}$, holding $\Delta\sigma$ constant, and integrating the Paris law equation (24) between the initial crack length a_0 and the length a_f at which fast fracture takes over gives

$$a_0^{(2-n)/2} - a_f^{(2-n)/2} = \left(\frac{n-2}{2}\right)\frac{C'\pi^{n/2}\,\Delta\sigma^n}{\Delta K_{-4}^n} N_f \tag{27}$$

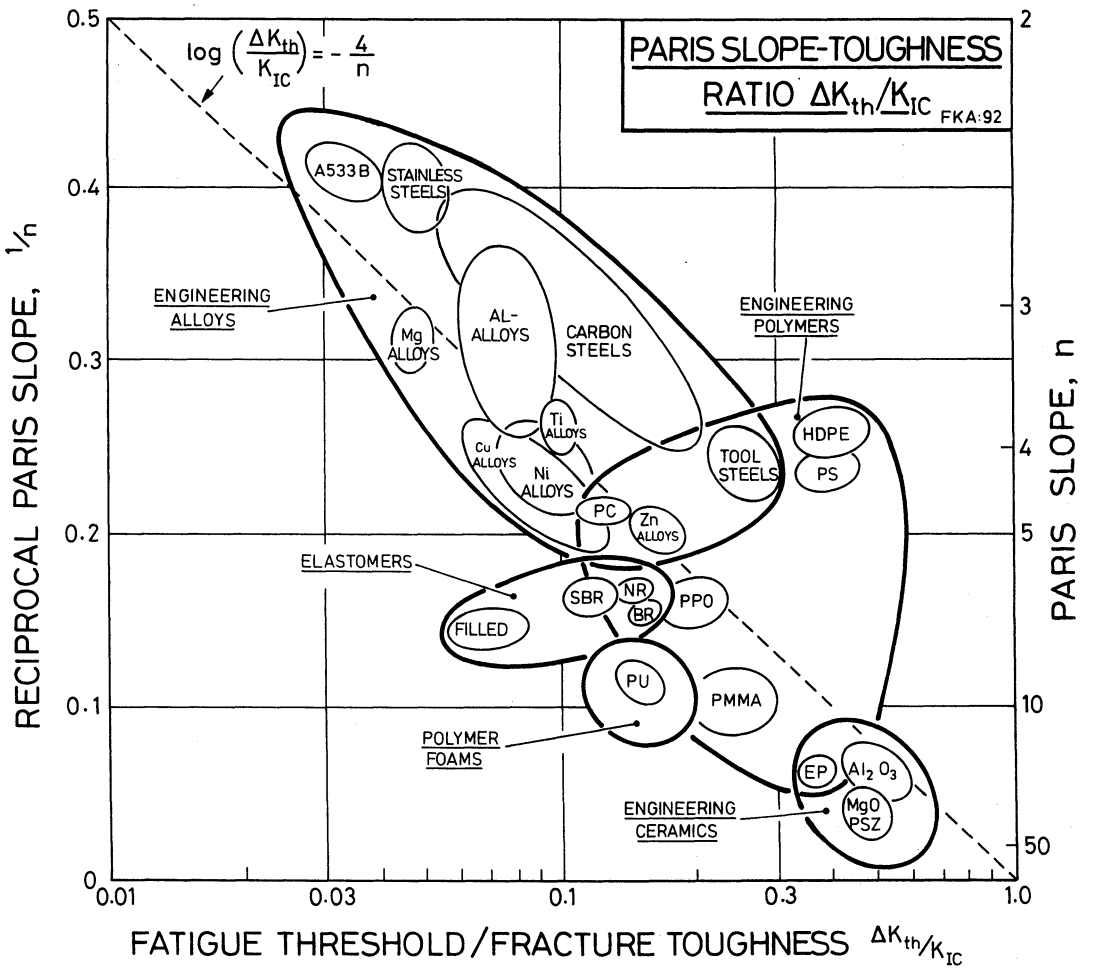

Fig. 16. The reciprocal Paris exponent, $1/n$, vs the ratio $\Delta K_{th}/K_{Ic}$. The diagonal contour is a plot of equation (12).

where a_0 is the initial flaw size, a_f is the final flaw size corresponding to catastrophic fracture $[a_f = (K_{Ic}^2/(\pi\Delta\sigma^2)]$ and N_f is the number of fatigue cycles to failure. Almost always, $a_f^{(2-n)/2} \ll a_0^{(2-n)/2}$, and the equation simplifies to

$$N_f = \frac{2}{n-2}\frac{a_0}{C'}\left(\frac{\Delta K_{-4}}{\Delta\sigma\sqrt{\pi a_0}}\right)^n \tag{28}$$

For a fixed life and stress amplitude

$$\log(\Delta K_{-4}) = \frac{\beta}{n} + \log(\Delta\sigma\sqrt{\pi a_0}) \tag{29}$$

where β, approximately a constant, is given by

$$\beta = \log\left(\frac{(n-2)C'N_f}{2a_0}\right). \tag{30}$$

The stress intensity range ΔK_{-4} and the reciprocal of the Paris index $1/n$, both measured at a crack growth rate of 10^{-4} mm/cycle, are shown graphically in Fig. 17. We note that n ranges from 2 to 40, and that ΔK_{-4} ranges from 0.01 to 50 MPa$\sqrt{\text{m}}$. Equation (29) has been used to add contours of constant stress range $\Delta\sigma$ to give a fatigue life of $N_f = 10^3$ cycles for an initial flaw size of $a_0 = 10$ mm; this value of a_0 is sufficiently large for linear elastic fracture mechanics to prevail at all stress levels of interest. It is evident from Fig. 17 that steels display the highest resistance and foams the lowest resistance to fatigue crack growth. The fatigue life shows little sensitivity to the value of n for $n > 4$ (that is, $1/n < 0.25$).

A common misconception is to assume that materials with the smallest value of n are the most fatigue resistant. That this is incorrect is simply demonstrated by considering two materials which possess the same ΔK_{-4} value but different n values. At applied ΔK levels below ΔK_{-4}, the material with the higher n value is the most fatigue resistant. The converse is true at applied ΔK levels above ΔK_{-4}.

6. CONCLUDING DISCUSSION

Material Property Charts have been constructed for fatigue. They are useful in showing fundamental relationships between fatigue and static properties, and in selecting materials for design against fatigue. One pair of charts displays the fatigue ratio, σ_e/σ_y and

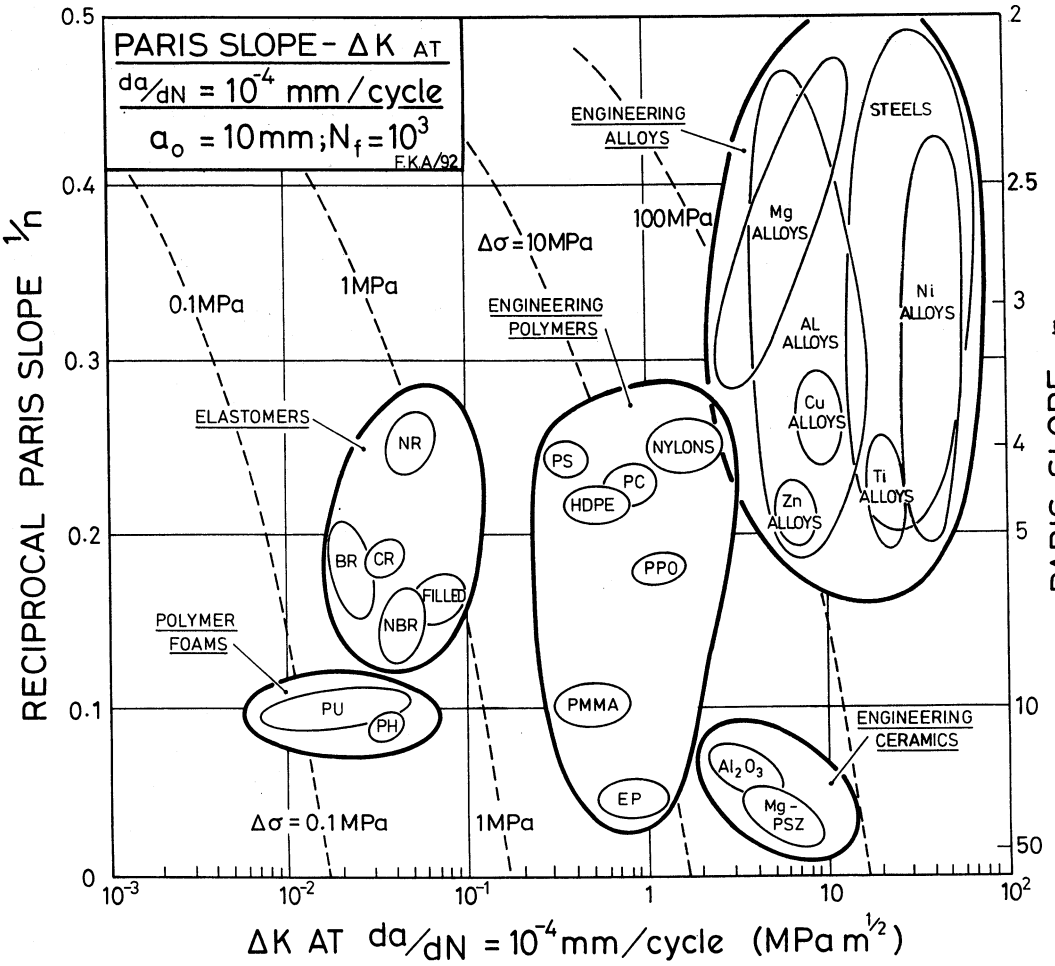

Fig. 17. The reciprocal Paris exponent, $1/n$, vs the stress intensity range ΔK_{-4} at a crack growth rate of 10^{-4} mm/cycle. Contours of stress range are shown for an initial crack length of 10 mm and a fatigue life of 10^3 cycles.

the fatigue-threshold ratio, $\Delta K_{th}/K_{Ic}$; they summarise the relative sensitivity of materials to cyclic loading. These two ratios vary widely from material class to class, making it important to use fatigue properties rather than monotonic properties in design for cyclic loading. Other charts show the process zone size in fatigue (it is smaller under cyclic loading than under monotonic loading) and the relative sensitivity of materials to cyclic crack growth. Still others relate fatigue properties to density, giving guidance in selection of materials for minimum-weight design under cyclic loading.

The presence of a notch in an engineering component encourages the initiation of a fatigue crack. A conservative approach is to design against initiation by ensuring that the local stress at the root of a notch is below the endurance limit of the material, but this approach is often too conservative to be cost-effective. Aircraft components, for example, are routinely designed for finite life, and a detailed knowledge of the crack initiation and the crack propagation responses are then required in order to design safely for minimum weight. Fatigue maps of the form shown in Figs 16 and 17 are a first step in seeking correlations for finite-life properties and in providing a tool for material selection at finite fatigue life.

Acknowledgements—K. J. Kang is grateful for financial support from Korean Science and Engineering Foundation in the form of a visiting scholarship. The authors wish to thank Mr D. A. Garton for help with initial data collection and software development, Dr G. J. Lake of Rubber Consultants for provision of data for several elastomers, and Professor L. M. Brown and Professor R. A. Smith for discussions on the modelling of the fatigue threshold. The financial support and continuing interest of Dr Steve Fishman, of the Office of Naval Research under Grant Number N00014-92-J-1805 is gratefully acknowledged.

REFERENCES

1. M. F. Ashby, *Acta metall.* **37**, 1273 (1989).
2. M. F. Ashby, *Materials Selection in Mechanical Design.* Pergamon Press, Oxford (1992).
3. S. Suresh, *Fatigue of Materials.* Cambridge Univ. Press (1991).

4. L. P. Pook. *The Role of Crack Growth in Metal Fatigue*. The Metals Society, London (1983).
5. J. A. Ewing and J. C. W. Humphrey, *Proc. R. Soc.* **A200,** 241 (1903).
6. A. T. Winter, *Phil. Mag.* **30,** 719 (1974).
7. C. Laird, *Mater. Sci. Engng* **22,** 231 (1976).
8. H. Mughrabi, *Mater. Sci. Engng* **33,** 207 (1978)
9. H. Mughrabi, *Proc. 5th Int. Conf. on Strength of Metals and Alloys* (edited by P. Haasen). Pergamon Press, Oxford (1979).
10. R. Wang, H. Mughrabi, S. McGovern and M. Rapp, *Mater. Sci. Engng* **65,** 219 (1984).
11. L. M. Brown, in *Material Behaviour and its Relation to Design* (edited by J. D. Embury and A. W. Thompson), pp. 175–199. ASM, Materials Park, Ohio (1990).
12. T. S. Sviram, M. E. Fine and Y. W. Chung, *Acta metall. mater.* **40,** 2769 (1992).
13. T. S. Sviram, C-M. Ke and Y. W. Chung, *Acta metall. mater.* **41,** 2515 (1993).
14. R. A. Smith, *Int. J. Fract.* **13,** R717 (1977).
15. K. J. Miller, *Proc. Inst. Mech. Engrs* **205,** 1 (1991).
16. R. W. Hertzberg and J. A. Manson, *Fatigue of Engineering Plastics*. Academic Press, New York (1980).
17. G. J. Lake and A. G. Thomas, *Proc. R. Soc.* **A300,** 108 (1967).
18. R. H. Dauskardt, D. B. Marshall and R. O. Ritchie, *J. Am. Ceram. Soc.* **73,** 893 (1990).
19. H. Kitakawa and S. Takahashi, *Proc. 2nd Int. Conf. on Mechanical Behaviour of Material*, pp. 627–631. ASM, Materials Park, Ohio (1967).